Green Chemistry

Supporting information for

Supercritical water hydrolysis: a pathway for producing low-molecular-weight cellulose

Jean Buffiere, Patrik Ahvenainen, Marc Borrega, Kirsi Svedström, and Herbert Sixta

Table of contents

1. MCC degradation kinetics

With a complete cellulose conversion within half a second, the experimental values for MCC conversion were in reasonable accordance with the results previously published using the shrinking core model. The numerical values for the reaction rate constants are shown in Table 1, while an Arrhenius plot is shown in Figure 1. The Arrhenius plot revealed a progressive decrease in the slope with increasing inverse temperature. This observation is compatible with previous results by Sasaki et al.[1] and Cantero et al.[2], who reported the presence of a break point in the reaction rate constants around the critical point. However, with an activation energy of 109 kJ.mol^{-1} calculated from the two lowest temperatures and of 170 kJ.mol-1 calculated from the two highest temperatures,

the shift observed in the present study was more gradual than previously recorded. A first reason is that the temperature range investigated was relatively narrow and thus possibly did not allow visualising the entire extent of the shift. A second reason to explain the differences in activation energies is that the MCC used in this study had a slightly different reactivity than that used by other authors. Tolonen et al.[3] showed that different types of MCCs can exhibit significant differences in their reactivity under similar hydrothermal conditions.

Table 1 Kinetic constants of cellulose degradation.

Temperature T (°C)	Reciprocal 1/T (K^{-1})	Kinetic constant k (-)	Log k (-)
360	1.5794	0.8306	-0.1856
370	1.5548	1.1454	0.1358
380	1.5310	1.6164	0.4802
387	1.5149	2.2516	0.8116

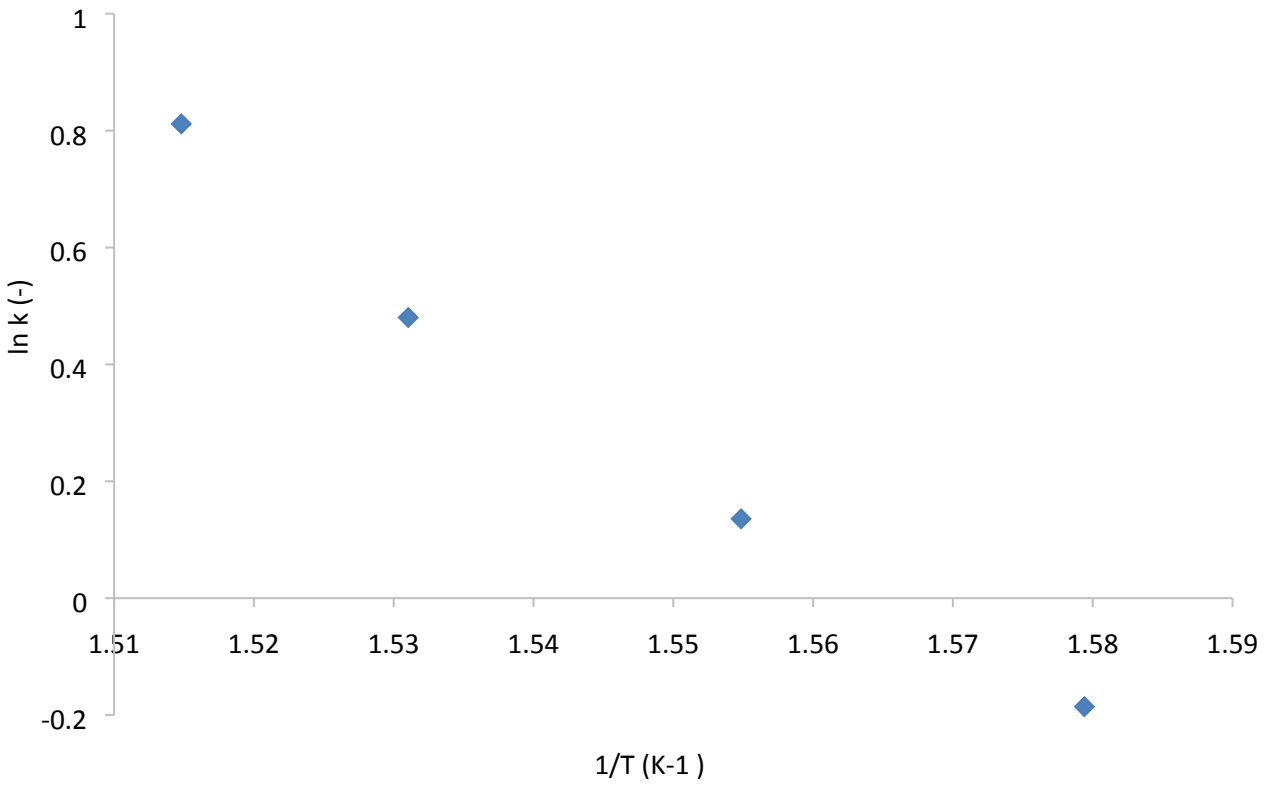

Fig. 1 Arrhenius plot of cellulose conversion using a shrinking core model.

2. Product mass balance

The numerical values as well as experimental error associated with the product mass balance presented in Figure 1 of the manuscript are shown in Table 2.

Table 2. Numerical values and experimental error (values in parentheses) for the product mass balance, expressed as percentage of the total product yield.

Temperature	Reaction time	Residue	WI-LMWC	WS-LMWC	Glucose	Other
360 °C	0.1 s	-	-	-	-	-
	0.2 s	64.4 (±0.2)	6.8 (±0.2)	15.4 (±7.0)	0.3 (±3.0)	13.2 (±10.4)
	0.3 s	54.3 (±0.2)	7.4 (±0.2)	21.7 (±7.0)	2.1 (±3.0)	14.5 (±10.4)
	0.4 s	24.4 (±0.2)	11.8 (±0.2)	36.9 (±7.0)	5.0 (±3.0)	21.8 (±10.4)
	0.5 s	0	9.4 (±0.2)	50.8 (±7.0)	11.3 (±3.0)	28.6 (±10.2)
	0.6 s	0	0	36.9 (±7.0)	16.8 (±3.0)	46.3 (±10.0)
370 °C	0.1 s	-	-	-	-	-
	0.2 s	58.6 (±0.2)	7.0 (±0.2)	17.8 (±7.0)	1.3 (±3.0)	15.2 (±10.4)
	0.3 s	40.2 (±0.2)	12.2 (±0.2)	28.5 (±7.0)	3.4 (±3.0)	15.7 (±10.4)
	0.4 s	7.7 (±0.2)	18.7 (±0.2)	38.2 (±7.0)	4.8 (±3.0)	30.7 (±10.4)
	0.5 s	0	7.6 (±0.2)	43.4 (±7.0)	8.2 (±3.0)	40.8 (±10.2)
	0.6 s	0	0	41.0 (±7.0)	12.5 (±3.0)	46.5 (±10.0)
380 °C	0.1 s	59.6 (±0.2)	5.5 (±0.2)	13.8 (±7.0)	0.7 (±3.0)	20.4 (±10.4)
	0.2 s	50.2 (±0.2)	5.9 (±0.2)	21.0 (±7.0)	2.6 (±3.0)	20.3 (±10.4)
	0.3 s	24.4 (±0.2)	11.9 (±0.2)	32.4 (±7.0)	4.8 (±3.0)	26.5 (±10.4)
	0.4 s	3.0 (±0.2)	17.2 (±0.2)	45.7 (±7.0)	6.9 (±3.0)	27.2 (±10.4)
	0.5 s	0	0.7 (±0.2)	43.0 (±7.0)	11.9 (±3.0)	44.3 (±10.2)
	0.6 s	0	0	31.9 (±7.0)	19.1 (±3.0)	49.0 (±10.0)
387 °C	0.1 s	33.8 (±0.2)	10.5 (±0.2)	25.7 (±7.0)	2.2 (±3.0)	27.8 (±10.4)
	0.2 s	27.3 (±0.2)	11.5 (±0.2)	30.6 (±7.0)	3.5 (±3.0)	27.0 (±10.4)
	0.3 s	11.7 (±0.2)	13.4 (±0.2)	35.1 (±7.0)	5.5 (±3.0)	34.3 (±10.4)
	0.4 s	0	0	35.9 (±7.0)	12.2 (±3.0)	51.9 (±10.0)

	0.5 s	0	0	27.3 (±7.0)	15.1 (±3.0)	57.8 (±10.0)
	0.6 s	0	0	11.6 (±7.0)	18.3 (±3.0)	70.1 (±10.0)

3. Molecular weights

The numerical values for the DPw and PDI of the residue and WI-LMWC fractions as shown in Figure 3 of the manuscript are shown in Table 3.

Table 3. Weight-average degree of polymerization (DP_w) as well as polydispersity index (PDI) of the residue and WI-LMWC. Values for MCC: DP_w = 380.3, PDI = 4.78.

Temperature	Reaction time	Residue		WI-LMWC	
		DP_w	PDI	DP_w	PDI
360 °C	0.1 s	-	-	-	-
	0.2 s	177.8	4.73	17.7	1.49
	0.3 s	145.1	4.49	18.1	1.53
	0.4 s	121.9	4.33	19.1	1.6
	0.5 s	38.4	2.62	16.8	1.5
	0.6 s	-	-	-	-
370 °C	0.1 s	-	-	-	-
	0.2 s	125.8	3.94	16.9	1.46
	0.3 s	111.3	4.22	18.7	1.55
	0.4 s	63.5	3.22	20.4	1.62
	0.5 s	-	-	16.8	1.51
	0.6 s	-	-	-	-
380 °C	0.1 s	161.7	4.59	17.2	1.44
	0.2 s	125.6	4.14	18.4	1.5
	0.3 s	117.6	4.57	19.9	1.58
	0.4 s	60.4	3.46	20.6	1.61
	0.5 s	-	-	-	-
	0.6 s	-	-	-	-
387 °C	0.1 s	86.9	3.28	19.4	1.51
	0.2 s	110.1	4.58	20.1	1.58
	0.3 s	96.8	4.25	20.8	1.58
	0.4 s	-	-	-	-
	0.5 s	-	-	-	-
	0.6 s	-	-	-	-

4. Energy demand

The detailed thermodynamic values used to calculate the energy demand are shown in Table 4. A value of 84 kJ.kg^{-1} was used for the specific enthalpy of pure water at 20 °C under a pressure of 0.1 MPa. In addition, the detailed experimental values used to calculate the energy demand is shown in Table 5.

Table 4. Thermodynamic values used for calculating the energy demand. The specific enthalpy of water was obtained from Lemmon et al.[4]

Reaction temperature	Preheated water temperature	Specific enthalpy of preheated water
°C	°C	kJ.kg^{-1}
360	419	2762
370	446	2930
380	499	3162
387	595	3479

Table 5. Experimental values used for calculating the energy demand.

#	T	t	Cellulose flow	Heating flow	Quenching flow	WI-LMWC conc.	WS-LMWC conc.	Glucose conc.	WI-LMWC conc.	WS-LMWC conc.	Glucose conc.
-	°C	s	kg/h	kg/h	kg/h	mg.kg^{-1}	mg.kg^{-1}	mg.kg^{-1}	g.h^{-1}	g.h^{-1}	g.h^{-1}
1	360	0.2	1.66	2.49	5.93	156.8	356.0	6.8	0.93	2.11	0.04
2	360	0.3	1.11	1.66	3.96	164.7	483.1	46.1	0.65	1.91	0.18
3	360	0.4	0.83	1.25	2.97	250.6	782.7	107.1	0.74	2.32	0.32
4	360	0.5	0.67	1.00	2.37	203.7	1102.3	244.3	0.48	2.62	0.58
5	360	0.6	0.55	0.83	1.98	0	730.6	332.7	0	1.45	0.66
6	370	0.2	1.53	2.29	5.79	148.7	378.0	28.6	0.86	2.19	0.17
7	370	0.3	1.02	1.53	3.86	228.9	533.7	63.7	0.88	2.06	0.25
8	370	0.4	0.76	1.14	2.90	346.4	706.1	88.8	1.00	2.04	0.26
9	370	0.5	0.61	0.92	2.32	150.4	857.2	161.1	0.35	1.98	0.37
10	370	0.6	0.51	0.76	1.93	0	826.9	251.8	0	1.60	0.49
11	380	0.1	2.45	3.68	9.98	114.5	284.6	14.2	1.14	2.84	0.14
12	380	0.2	1.23	1.84	5.04	109.1	389.0	48.7	0.55	1.96	0.25
13	380	0.3	0.82	1.23	3.36	217.9	592.9	87.1	0.73	1.99	0.29
14	380	0.4	0.61	0.92	2.52	299.6	796.4	121.0	0.75	2.01	0.30
15	380	0.5	0.49	0.74	2.02	12.8	747.6	207.1	0.03	1.51	0.42
16	380	0.6	0.41	0.61	1.68	0	522.6	312.1	0	0.88	0.52
17	387	0.1	1.58	2.37	7.15	184.0	449.1	38.1	1.32	3.21	0.27
18	387	0.2	0.79	1.18	3.58	166.1	441.5	49.9	0.59	1.58	0.18
19	387	0.3	0.53	0.79	2.39	208.7	548.8	86.6	0.50	1.31	0.21
20	387	0.4	0.39	0.59	1.79	0	579.0	196.2	0	1.04	0.35

21	387	0.5	0.32	0.47	1.43	0	429.8	238.2	0	0.62	0.34
22	387	0.6	0.26	0.39	1.19	0	165.1	261.0	0	0.20	0.31

5. References

1 M. Sasaki, T. Adschiri and K. Arai, *AIChE J.*, 2004, **50**, 192–202.

2 D. A. Cantero, M. D. Bermejo and M. J. Cocero, *J. Supercrit. Fluids*, 2013, **75**, 48–57.

3 L. K. Tolonen, P. A. Penttilä, R. Serimaa and H. Sixta, *Cellulose*, 2015, **22**, 1715–1728.

4 E. W. Lemmon, M. O. McLinden and D. G. Friend, in *NIST Chemistry WebBook, NIST Standard Reference Database Number 69*, eds. P. J. Linstrom and W. G. Mallard, National Institute of Standards and Technology.